

decouple the  $^{31}\text{P}$  signal would be a time-consuming process (because of the large chemical shift range of  $^{57}\text{Fe}$ ), we have found that a correlation exists between the  $^{31}\text{P}$  and the  $^{57}\text{Fe}$  chemical shifts, as shown in Figure 2. This correlation makes it easy to predict the  $^{57}\text{Fe}$  chemical shift of a new complex, thus simplifying the search for the proper decoupling frequency and allowing determination the  $^{57}\text{Fe}$  chemical shift of a new complex in about 20 min.

Replacement of electron-withdrawing groups, Cl, by electron-donating groups,  $\text{OCH}_3$ , at the para positions of the phenyl rings of TPP causes shifts of  $^{57}\text{Fe}$  and  $^{31}\text{P}$  resonances to lower shielding, as summarized in Figure 2. (Actual chemical shifts and coupling constants are given in the supplementary material, Table S-1.) For the  $^{57}\text{Fe}$  case, this is the predicted direction, based on the paramagnetic contribution to the screening constant being the dominant factor for heavy nuclei, especially those with unfilled d-shells such as these low-spin  $d^6$  complexes.<sup>20</sup> The spread of the  $^{57}\text{Fe}$  shifts is somewhat larger than that of the  $^{59}\text{Co}$  chemical shifts reported earlier for the same series of para-substituted  $[\text{TPPCo}(\text{NMeIm})_2]^+$  complexes.<sup>21</sup> Substitution of one  $\text{PMe}_3$  by CO, both good  $\pi$ -acids,<sup>22</sup> yields a similar  $^{57}\text{Fe}$  chemical shift (but a smaller  $^{31}\text{P}$  chemical shift), while substitution by a number of aromatic and aliphatic amines or benzyl methyl sulfide shifts the iron resonance to lower shielding by  $\sim 1200$  ppm. The isonitrile ligand is expected to be a good  $\sigma$ -donor but a poorer  $\pi$ -acceptor than CO or the phosphine,<sup>22</sup> consistent with its intermediate  $^{57}\text{Fe}$  and  $^{31}\text{P}$  chemical shifts. *N*-Methylimidazole,<sup>23</sup> 4-(dimethylamino)pyridine,<sup>23</sup> and benzyl methyl sulfide are expected to be both good  $\sigma$ - and  $\pi$ -donors, while 4-cyanopyridine<sup>23</sup> is expected to be a weak  $\sigma$ -donor and fairly good  $\pi$ -acceptor and *N*-butylamine is only a  $\sigma$ -donor, yet they all display fairly similar  $^{57}\text{Fe}$  and  $^{31}\text{P}$  shifts. The observed relationship between  $^{57}\text{Fe}$  and  $^{31}\text{P}$  chemical shifts (Figure 2) suggests a possible synergism in the  $\sigma$ - and  $\pi$ -bonding effects of phosphine–L trans axial ligand combinations, such that when a strong  $\sigma$ - or  $\pi$ -donor ligand is present trans to a phosphine, it has the effect of decreasing the shielding of both the metal and the phosphine nuclei. (However, the effect is not a simple one, since the trend among the three pyridines is the reverse of that expected in terms of either  $\sigma$ - or  $\pi$ -donor characteristics, i.e.,  $\delta(4\text{-NMe}_2\text{Py}) < \delta(\text{Py}) < \delta(4\text{-CNPY})$ .) The increase in coupling constants  $J_{\text{Fe-P}}$  upon a change in L from CO (36 Hz) to the nitrogen donors and the thioether (47–59 Hz) (Table S-1) also suggests synergism in the  $\sigma$ - and  $\pi$ -bonding of these ligand combinations. Investigations of additional mixed-ligand complexes aimed at probing the factors that affect the  $^{57}\text{Fe}$  and  $^{31}\text{P}$  chemical shifts and the coupling constants are underway.

The temperature dependences of the  $^{57}\text{Fe}$  and  $^{31}\text{P}$  chemical shifts were investigated over the range  $-61$  to  $+30$  °C in toluene- $d_6$  and from 20 to 55 °C in benzene- $d_6$ . Linear shifts of both resonances with temperature were observed, with the  $^{57}\text{Fe}$  and  $^{31}\text{P}$  chemical shifts having opposite temperature dependences (Table S-1). Both  $[\text{TPPZnPMe}_3]$  and  $\text{PMe}_3$  itself also display smaller shifts of the  $^{31}\text{P}$  signal to higher shielding with increasing temperature ( $-0.014$  and  $-0.005$  ppm/°C, respectively), and a similar temperature dependence of the  $^{31}\text{P}$  chemical shifts has been reported for a series of dimeric Pd(I) complexes of the type  $[\text{Pd}_2(\text{dppm})_2\text{X}_2]$ .<sup>24</sup> Neither  $^{31}\text{P}$  nor  $^{57}\text{Fe}$  chemical shifts were concentration dependent over the range 6–24 mM. Solvent effects are also very small.

Most model hemes and heme proteins investigated thus far,<sup>5–11</sup> including those presented in Table S-1, have  $^{57}\text{Fe}$  chemical shifts ranging from 7200 to 9200 ppm vs  $\text{Fe}(\text{CO})_5$ . However, the  $^{57}\text{Fe}$

resonance of cytochrome *c* is observed at 11197 ppm,<sup>4</sup> which is dramatically shifted to lower shielding by 3000. Due to this dramatic shift for the cytochrome *c* resonance, we had anticipated that the thioether complex of our study would display an  $^{57}\text{Fe}$  chemical shift significantly different from that of the *N*-methylimidazole and other nitrogen donor complexes. However, this is not the case (Figure 2). We thus suggest that the unusual  $^{57}\text{Fe}$  chemical shift of cytochrome *c*<sup>4</sup> may include a contribution not found in model hemes: the contribution of fixed axial ligand orientation. In model hemes at ambient temperatures, axial ligands are expected to rotate rapidly. We are currently investigating specially designed model heme complexes in which axial ligand rotation is hindered in order to determine the effect of fixed axial ligand plane orientation on the  $^{57}\text{Fe}$  and  $^{31}\text{P}$  chemical shifts and chemical shift anisotropies.

**Acknowledgment.** The financial support of the National Institutes of Health (DK 31038) is gratefully acknowledged. The authors also wish to thank Professor Richard S. Glass for supplying the sample of benzyl methyl sulfide and Professor David E. Wigley for providing the cylinder of CO.

**Supplementary Material Available:** A table of  $^{57}\text{Fe}$  and  $^{31}\text{P}$  chemical shifts of Fe(II) tetraphenylporphyrins bound to trimethylphosphine (Table S-1) (1 page). Ordering information is given on any current masthead page.

### Experimental Evidence by EXAFS of the Second Hydration Shell in Dilute Solutions of $\text{Cr}^{3+}$

Adela Muñoz-Paez\*<sup>†</sup> and Enrique Sánchez Marcos<sup>‡</sup>

Departamento de Química Inorgánica e Instituto de Ciencias de Materiales, Facultad de Química Universidad de Sevilla, 41012-Sevilla, Spain  
Departamento de Química Física, Facultad de Química Universidad de Sevilla, 41012-Sevilla, Spain

Received March 30, 1992

Since Frank and Evans<sup>1</sup> proposed their concentric shell model, concepts of the first and second hydration shell have been widely used for understanding the structure of solvated ions and, as a consequence, the rationalization of a large number of chemical properties of electrolyte-containing solutions.<sup>2</sup> Direct experimental evidence of ionic solution structure has been obtained from X-ray and neutron diffraction.<sup>3</sup> In particular, a description of the first hydration shell for a large number of monoatomic cations and anions has been reported;<sup>4</sup> however, for the second hydration shell, available information is not so general. An important limitation of these techniques is that the species to be studied must be quite concentrated, namely, up to 1.0 M.

Information about the local environment around cations in highly dilute solutions (ca.  $10^{-3}$  M) can be obtained by the EXAFS technique (extended X-ray absorption fine structure), which is an excellent tool to study short-range order about a specific type of atom. This technique has allowed us to examine an experimental system closer to the ideal concept of infinitely dilute solutions, where the ion–solvent interactions are not disturbed by the ion–ion interactions. Decrease of sensitivity of the absorber–backscatterer distance inherent in this technique has precluded, until now, the unambiguous determination of the second

(20) Laszlo, P. In *NMR of Newly Accessible Nuclei*; Laszlo, P., Ed.; Academic Press: New York, 1983; Vol. 2, pp 259–266.

(21) Hagen, K. I.; Schwab, C. M.; Edwards, J. O.; Jones, J. G.; Lawler, R. G.; Sweigart, D. A. *J. Am. Chem. Soc.* 1988, 110, 7024.

(22) Cotton, F. A.; Wilkinson, G. *Advanced Inorganic Chemistry*, 5th ed.; Wiley Interscience: New York, 1988; pp 57–68.

(23) (a) Safo, M. K.; Gupta, G. P.; Watson, C. T.; Simonis, U.; Walker, F. A.; Scheidt, W. R. *J. Am. Chem. Soc.*, in press. (b) Lichtenberger, D. L.; Walker, F. A.; Gruhn, N. E.; Bjerke, A. Manuscript in preparation.

(24) Hunt, C. T.; Balch, A. L. *Inorg. Chem.* 1982, 21, 1641–1644.

(25) The 5-mm  $^{57}\text{Fe}$ ,  $^1\text{H}$ ,  $^{31}\text{P}$  probe was purchased from Cryomagnet Systems, Inc., Indianapolis, IN.

<sup>†</sup> Departamento de Química Inorgánica e Instituto de Ciencias de Materiales.

<sup>‡</sup> Departamento de Química Física.

(1) Frank, H. S.; Evans, M. W. *J. Chem. Phys.* 1945, 13, 507.

(2) Marcus, Y. *Ion Solvation*; Wiley: Chichester, 1986. Marcus, Y. *Chem. Rev.* 1988, 88, 1475.

(3) Burgess, J. *Ions in Solution*; Ellis Horwood: Chichester, 1988.

(4) Magini, M.; Licheri, G.; Paschina, G.; Piccaluga, G. *X-ray Diffraction of Ions in Aqueous Solutions: Hydration and Complex Formation*; CRC Press: Boca Raton, FL, 1988.

**Table I.** Fitting Parameters for the EXAFS Spectra of a Cr<sup>3+</sup> Aqueous Solution (10<sup>-2</sup> M)<sup>a</sup>

	<i>N</i>	$\Delta\sigma^2$ (Å <sup>2</sup> )	<i>R</i> (Å)	$\mathcal{E}_0$ (eV)
Cr-O <sub>1</sub>	6.0 ± 0.1	0.0000 ± 0.0005	2.00 ± 0.01	1.1 ± 0.3
Cr-O <sub>2</sub>	13.5 ± 1.2	0.0108 ± 0.0035	4.02 ± 0.02	1.0 ± 0.7

<sup>a</sup>*N* = number of neighboring atoms;  $\Delta\sigma^2$  = Debye-Waller factor; *R* = absorber-backscatterer distance; O<sub>1</sub> and O<sub>2</sub> coming from the water molecules of the first and second hydration shells, respectively; and  $\mathcal{E}_0$  = threshold energy or inner potential.

hydration shell. The aim of this work has been to obtain experimental information on this shell for dilute solutions. Therefore, we have undertaken the study by EXAFS of the solvent structure around Cr<sup>3+</sup> in 10<sup>-2</sup> M aqueous solution. This cation was chosen since its high charge, small size, and large mean residence time of water molecules in the first hydration shell are factors that should favor a well-defined second hydration shell. Evidence of the existence of a second shell for more concentrated Cr<sup>3+</sup> aqueous solutions (ca. 1 M) has been previously reported, using XRD<sup>5</sup> and IR spectroscopy.<sup>6</sup>

Cr K-edge spectra of Cr(NO<sub>3</sub>)<sub>3</sub> solutions (10<sup>-2</sup> M) were measured at the SRS (Daresbury, U.K.) in the fluorescence mode in a specially adapted liquid cell.<sup>7</sup> Cr(NO<sub>3</sub>)<sub>3</sub>·9H<sub>2</sub>O salt (Merck P.A.) was used to prepare the solution.

The radial distribution function obtained from the *k*<sup>2</sup> weighted Fourier transform<sup>8</sup> ( $\Delta k = 2.72$ – $11.80$  Å<sup>-1</sup>) of the EXAFS function  $\chi(k)$  shows two well-resolved peaks, the first centered at 2.0 Å and the latter, approximately one-fourth the intensity of the former, centered at 4.0 Å. They can be assigned to the first and second hydration shells, respectively. Data analysis<sup>9</sup> of the EXAFS spectrum was performed in *k* and *R* space using the phase shift and backscattering amplitude functions determined from the spectrum of crystalline Cr(NO<sub>3</sub>)<sub>3</sub>·9H<sub>2</sub>O.<sup>10</sup> A fairly good reproduction of the experimental data (fit variance  $6 \times 10^{-3}$ ) was obtained with a two-shell fit. Comparative plots of the best fit (dotted line) and the experimental EXAFS function (solid line) appear in Figure 1. Fit parameters and standard deviations appear in Table I.

Since eight free parameters (*P*) were used in the fit (2 shells × 4 parameters/shell) and the total number of independent points is 22 ( $N_{\text{pts}} = (2\Delta k\Delta R)/\pi + 1$ ),<sup>11</sup> the degree of freedom of the fit ( $\nu = N_{\text{pts}} - P$ ) is 14, a number high enough to obtain reliable results. Moreover, the parameters are not really free to move. Thus, according to the information obtained by XRD for more concentrated solutions,<sup>5</sup> the number of water molecules in the first hydration shell should be around 6, this number not being expected to be affected by dilution. Thus, this parameter could vary within a narrow range (parameter constraint 5–7). Likewise, the coordination number for the second hydration shell was kept at around 12 (parameter constraint 10–14). Since  $\Delta\sigma^2$  and *N* are coupled,<sup>4,12</sup> once the *N* value is fixed, an estimate of Debye-Waller factors relative to the hydrated crystal, used as a reference, is obtained. In contrast with this, when absolute values of the distance Cr–O in the hydrated crystal are known,<sup>10,12</sup> results of the fit provide an accurate description of coordination distances, 2.00 and 4.02 Å for the first and second hydration shells, re-

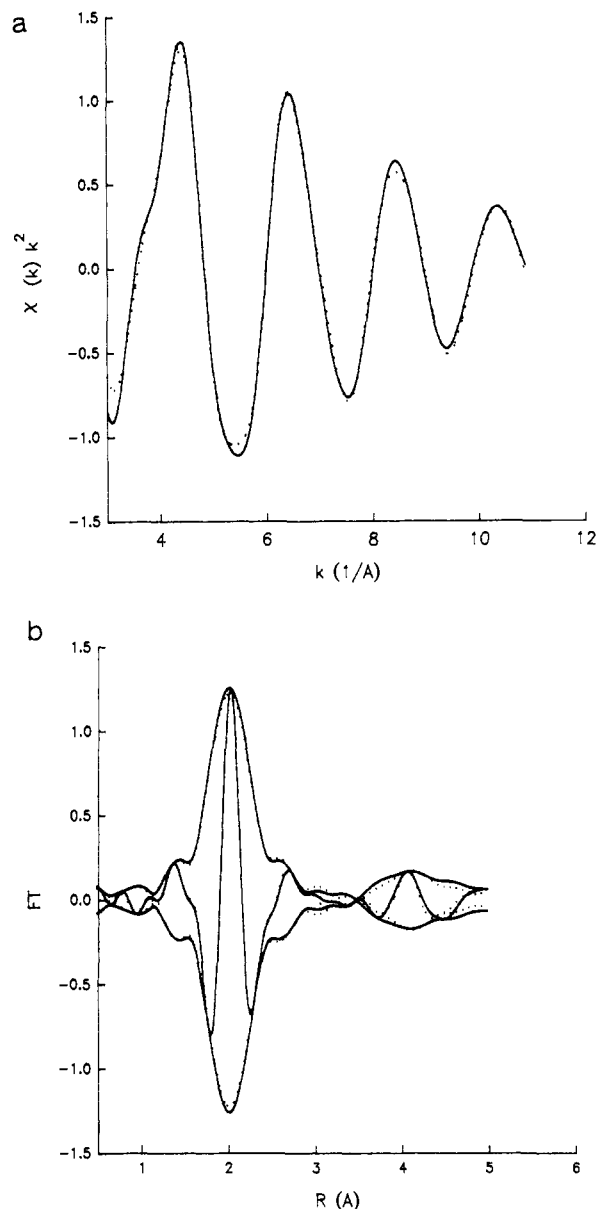


**Figure 1.** (a) Fourier filtered experimental data ( $k^2$ ,  $\Delta k = 2.7$ – $11.8$  Å<sup>-1</sup>,  $\Delta R = 0.3$ – $4.2$  Å) (solid line) and the best fit (dotted line). (b) Absolute and imaginary part of Fourier transform ( $k^2$ ,  $\Delta k = 3$ – $10.7$  Å) of the curves included in part a, corrected for Cr–O phase shift.

spectively. A second hydration shell was observed when the EXAFS spectra of more concentrated chromium solutions<sup>13</sup> were analyzed.

Although quantitative analysis of the EXAFS signal has been carried out, the main contribution of the present work is to give direct qualitative evidence of the existence of a second hydration shell around Cr<sup>3+</sup> ions in dilute aqueous solutions. We believe that this result may stimulate other groups to further efforts in the research of the structure of highly dilute aqueous solutions by EXAFS.

**Acknowledgment.** Thanks are due to DL for an allocation of beam time (BAP 20) and to the staff there for helping during the measurements, especially to M. Oversluizen. We are indebted as well to D. C. Koningsberger and M. Vaarkamp for the use of their EXAFS analysis programs. The Spanish DGICYT is acknowledged for financial support (PB89-0642).

**Registry No.** Cr(H<sub>2</sub>O)<sub>6</sub><sup>3+</sup>, 14873-01-9.

(5) Caminiti, R.; Licheri, G.; Piccaluga, G.; Pinna, G. *J. Chem. Phys.* **1976**, *65*, 3134; **1978**, *69*, 1.

(6) Bergström, P. A.; Lindgren, J.; Read, M.; Sandström, M. *J. Phys. Chem.* **1991**, *95*, 7650.

(7) Measurements were carried out at Station 8.1, using a double crystal monochromator, Si[220], with 30% HHR and a Canberra multielement detector. The ring conditions used were 2 GeV and 250 mA. A liquid cell, SPECAC 7500, with variable path length, 0–6 mm, was modified, substituting NaCl windows by Mylar films. Design of the Teflon O-rings for the cell was kindly supplied by F. Villain from LURE (Orsay, France).

(8) Normalization was done by dividing by the height of the absorption edge, and the background was subtracted using cubic spline routines. Noise level is around 0.004 in the averaged EXAFS spectra.

(9) Duivenvorden, F. M. B.; Koningsberger, D. C.; Uh, Y. S.; Gates, B. C.; *J. Am. Chem. Soc.* **1986**, *108*, 6254.

(10) Kannan, K. K.; Viswamitra, M. A. *Acta Crystallogr.* **1965**, *19*, 151.

(11) Lytle, F. W.; Sayers, D. E.; Stern, E. A. *Physica B* **1989**, *158*, 701.

(12) Sakane, H.; Miyayama, T.; Watanabe, I.; Yokoyama, Y. *Chem. Lett.* **1990**, 1623.

(13) [Cr<sup>3+</sup>] = 10<sup>-1</sup> and 5 × 10<sup>-2</sup> M prepared from nitrate and chloride salts and measured in the transmission mode. Muñoz-Paez, A.; Sanchez Marcos, E. To be published.